Canadian Science Publishing | Canadian Journal of Civil Engineering

# Evaluation of top-down crack propagation in asphalt pavement under dual tires loading

| | |
|---|---|
| Journal: | *Canadian Journal of Civil Engineering* |
| Manuscript ID | cjce-2018-0432.R1 |
| Manuscript Type: | Article |
| Date Submitted by the Author: | 19-Dec-2018 |
| Complete List of Authors: | Alae, Mohsen; Dalian University of Technology<br>Haghshenas, Hamzeh F.; Nebraska Department of Transportation<br>Zhao, Yanqing; Dalian University of Technology |
| Keyword: | crack propagation, top-down cracking, finite element method, stress intensity factor, asphalt pavement |
| Is the invited manuscript for consideration in a Special Issue? : | Not applicable (regular submission) |
| | |

# Evaluation of top-down crack propagation in asphalt pavement under dual tires loading

Mohsen Alae[1]; Hamzeh F. Haghshenas[2]; Yanqing Zhao[3]

[1]Research Assistant, School of Transportation Engineering, Dalian University of Technology, Dalian 116024, China. Email: mohsen_374@yahoo.com

[2]Materials and Research Engineer, Nebraska Department of Transportation (NDOT), 1400 Highway 2, Lincoln, NE 68509, USA. Email: hamzeh.haghshenas@nebraska.gov

[3]Professor, School of Transportation Engineering, Dalian University of Technology, Dalian 116024, China, telephone number: (+86) 15804269202, Email (corresponding author): yanqing_zhao@dlut.edu.cn

**Abstract:** Top-down cracking (TDC) has been recognized worldwide and is regarded as a major type of asphalt pavement distress. In this study, fracture mechanisms behind the TDC propagation and fatigue life of pavements were investigated under dual tires load using finite element (FE) analysis. By considering the most influencing factors on TDC propagation, stress intensity factors (SIF), including KI and KII, were calculated at critical transverse locations. According to Modes I and II SIF, a greater SIF indicates a faster rate of TDC propagation. The SIF results indicated that considering temperature gradient in asphalt concrete (AC) layer is necessary in determination of critical SIF, and KI and KII are not distributed uniformly within the AC depth. In addition, TDC growth rate significantly depends on AC thickness and base layer type. Finally, the number of load repetitions for TDC propagation rate at different transverse locations is predicted based on Paris law equation.



**Keywords:** crack propagation; top-down cracking; finite element method; stress intensity factor; asphalt pavement

## Introduction

Conventionally, it is assumed that fatigue cracking, as a well-known mode of asphalt pavement distress, is initiated from the bottom of the asphalt concrete (AC) layer and propagated towards the surface. However, recent findings revealed that Top-down fatigue cracking is a major type of asphalt pavement distress, which is initiated from the surface and propagated downward (Svasdisant et al. 2002; Sun et al. 2005; Zhao et al. 2018). Field investigation has shown that most top-down cracks (TDCs) are longitudinal and located in the vicinity of the wheel paths (Matsuno and Nishizawa 1992; Niderquell et al, 2000). TDC occurs in pavement due to various factors, including the tire-pavement contact stresses, modulus gradient due to the temperature and aging in AC layer, moduli of the base layers, and pavement structures (Ling et al. 2017a; wang et al. 2013; Svasdisant et al. 2002).

The pavement performance is directly related to the mechanisms of TDC propagation which is not completely clear yet. Considering all these influencing factors is necessary, not only for identification of crack propagation mechanism, but also for estimating the suitable rehabilitation and service life of the pavements. However, Ling et al. (2017a) demonstrated that field aging of AC layers is non-uniform along the pavement depth which results in higher modulus near the pavement surface and cannot be simulated or analyzed in laboratory, there are still controversial issues which are needed to consider in aging investigations in the field, such as polymer modified asphalt mixture, different climate regions and long-term aging effects (Li et al. 2006; Zhao and Wang, 2018).



The common parameters for evaluation of the fracture resistance in asphalt pavements include the stress intensity factors (SIF) (Jacobs et al. 1996; Modarres and Shabani, 2015), energy release rate or fracture energy (Bayomi et al. 2006); and J-integral (Ling et al. 2017b). However, the energy term J-integral is more appropriate for evaluation of crack propagation in viscoelastic materials and most of recent studies considered the elastic modulus in AC layer for J-integral calculations (Ling et al. 2017b; Lou et al. 2018). They have mentioned that it is impractical to run many calculations and change the Prony series parameters for the relaxation modulus in the finite element method (FEM). In addition, the fracture behaviour of AC layer depends on the geometry of a flaw, the stress state at the flaw and the loading mechanism around the flaw. Therefore, it is important to investigate the severity and stability of a crack by calculating SIF (K) which is a measure of stress state at the crack tip. The three SIF modes, KI, KII and KIII, are known in the fracture mechanics that are assigned to crack opening, sliding and tearing modes, respectively (Ameri et al. 2011).

In order to investigate the crack growth in asphalt materials under tension, three-point bending beam and four-point loading techniques have been generally employed (Molenaar et al. 2003; Kim et al. 2009; Huang et al. 2013). In most of previous studies, the crack growth rate has been examined under tensile stress whereas the cracks at the pavement surface experience tensile and shear deformations; this leads to TDC propagation due to the shear mode and/or the combination of tensile-shear mode. However, Aliha et al. (2016) carried out experimental tests for evaluating the mixed Mode I and III of fracture toughness in asphalt mixture, they revealed that there are several difficulties to compute the fracture parameters (combination of Modes I and III) of the real pavements due to the complicated geometry and loading type. It is worthy of note that numerical analysis, such as finite element (FE) and finite difference (FD), is a powerful technique for the study of crack propagation (Shen et al. 2016). For instance, Roesler and Khazanovich (1997) estimated the SIFs of a partial-depth crack in a Portland cement concrete pavement by using FE technique. In addition, the effect of vehicle's speeds on SIF have been analyzed at the crack tip based on the numerical analysis (Zhao et al. 2011; Yang et al. 2011).

Many studies have been also devoted to the identification of the mechanisms behind TDC propagation in pavements. Myers and Roque (2002) evaluated the influence of temperature gradient on TDC propagation at the crack tip via finite element (FE) method. Using coupled element free Galerkin (EFG) and FE method, Luo et al. (2010) concluded that

TDC propagation rate is significantly affected by the stiffness of AC and base layer. Fakhri et al. (2009) studied the single tire load effects on Modes I and II of fracture parameters. In another study, Ameri et al. (2011) analyzed the propagation of transverse crack at the pavement surface by considering a moving load with respect to the crack.

Using Extended Finite Element Modeling concept (XFEM), the dependency of crack pattern on the location of the pre-existing cracks was elucidated under single tire loading (Rashadul Islam et al. 2016). However, in this work, only the effect of crack distance from the loading center was regarded in the crack propagation.

A survey on previous literature indicates that only the effect of single tire load on TDC propagation has been considered in many published works; it should be pointed out that the single tire results in significantly less surface-initiated cracking compared to that of dual tires (Al-Qadi et al. 2004). In addition, the frequency of TDC is less in the case of single tires because TDC only initiates at or near the tire edges. However, the mechanisms of TDC initiation and propagation may not be identical, significant analyses are needed into better understanding the dual tires loading effects on the TDC propagation.

Furthermore, considering transverse crack at the pavement surface in study of TDC propagation rate (Holewinski et al, 2003; Ameri et al. 2011) may not be accurate assumption, because TDC manifests as a longitudinal crack induced by traffic loads near the tire edge (Wang 2009; Zhao et al. 2018) while transverse cracks are induced by thermal loads.

**Objective**

The primary objective of this study was, thus, to investigate the mechanisms of longitudinal TDC propagation based on dual tires load. In this regard, the effect of different factors including vehicle speed (loading frequency), temperature, crack position, crack depth, AC thickness and base layer type were evaluated on Modes I and II stress intensity factor (KI, KII) using numerical analyses. Furthermore, the critical conditions corresponding to TDC growth were identified. According to the obtained results, the fracture parameters (KI, KII) were correlated to pavement fatigue life in terms of the number of load repetition to the propagation of TDC.

## Methodology

In this paper, the typical pavement structures listed in Table 1 are considered as the FE models. To investigate the influence of dual tires loading on TDC propagation through the depth of AC layer, the crack plane is assumed normal to the traffic direction. This assumption results in Modes III SIF (tearing mode, KIII) to be insignificant or may not occur (Elseifi et al. 2018). Therefore, plane strain approach with 8-node elements (CPE8R) is used in the ABAQUS software for the pavements consisting of different crack depths, to analyze the effect of Modes I and II loading. In order to estimate the SIFs, fine meshes and singular (quarter point) elements were used in the stress field around crack tips. The bottom of FE model was considered fixed at all directions and the roller support was assigned to vertical boundaries of the model as the boundary conditions. Fully bonded interface conditions were assumed between the layers. The ABAQUS pavement model with the corresponding FE mesh and boundary conditions is shown in Figure 1 under dual tires loading; also, a close view of longitudinal TDC at the pavement surface is depicted in the figure.

Since the mechanical properties of AC vary significantly with temperature and loading frequency, the dynamic modulus master curve is usually used to characterize the behaviour of AC. According to AASHTO TP 62-07 (AASHTO 2007), the complex moduli were measured at six temperatures (-10, 0, 15, 30, 40 and 55°C) and six frequencies (20, 10, 5, 1, 0.5 and 0.1 Hz). In this study, the equivalent elastic moduli were determined by fitting the dynamic modulus data to the sigmoidal function on the basis of the time-temperature superposition principle. It should be noted that the recent studies have demonstrated that it is impractical to run many calculations and change Prony series parameters for the relaxation modulus in the FEM (Ling et al. 2017b; Lou et al. 2018). More than that, Roque et al. (2017) stated that the equivalent elastic modulus determined from master curve has the high level of accuracy as viscoelastic responses. Therefore, the equivalent elastic moduli determined at different temperatures were directly considered in ABAQUS as the AC layer moduli. Figure 2 shows the variation of equivalent elastic modulus of a typical frequency at 5Hz with temperatures. However, the determination of frequency in pavement structure is a subject of controversy in recent years (ARA 2004; Al-Qadi et al. 2008). The rate of loading (loading frequency) depends on the duration of the stress pulse. The pulse duration was determined using the equation (1) suggested in mechanistic-empirical pavement design guide (MEPDG):

$$t = \frac{L_{eff}}{17.6v_s} \tag{1}$$

Where $t$ is the pulse duration (s); $L_{eff}$ is the effective length (m); $v_s$ is the vehicle speed (m/s). The loading frequency was then estimated as the reciprocal of $t$.

To determine $L_{eff}$, the Odemark's method of equivalent thickness was adopted in the MEPDG to transform the pavement layers above the subgrade into one layer. The stress distribution lines in the transformed pavement were at 45 degrees, and thus the effective length at any depth could be calculated. Details about the determination of $L_{eff}$ are documented elsewhere (ARA 2004). Furthermore, the AC layers were divided into different sublayers and the loading frequency of each sublayer was determined according to the procedure mentioned previously. The equivalent elastic moduli at various temperatures and vehicle speeds were considerd for each sublayer from the dynamic modulus master curve and time-temperature shift factor.

It should be noted that temperature and its corresponding modulus of the asphalt layer is not uniform within the pavement depth (Archilla, 2015; Raju et al, 2008). As a result, for the AC layer with a stiffness gradient, the equivalent elastic modulus is calculated through the following equation from (Huang, 2004; Roque et al. 2017):

$$E_{eq} = \left[\frac{\sum_{i=1}^{n} h_i \cdot (E_i)^{1/3}}{\sum_{i=1}^{n} h_i}\right]^3 \quad (2)$$

where $h_i$ and $E_i$ are the thickness and modulus of the different sub-layers within the AC layer.

These equivalent elastic moduli of the sublayers were used in linear elastic theory (LET) to calculate the stress intensity factors ($K$I, $K$II). These factors are descriptive of crack tip stress states and conditions, and they were calculated separately using a contour-integral based method in ABAQUS. In order to obtain the critical parameters of TDC propagation in pavement, different transverse locations, ranging from the middle point of the dual tires to a distance of 250 cm, were regarded. The applied loads were dual tires with a magnitude of 0.7 MPa and a radius of 10 cm. The center-to-center distance of the dual tires was 30 cm.

The crack propagation rate in pavement structures was calculated using Paris law model in terms of equivalent SIF ($\Delta K_{eq}$) (Paris and Erdogan 1963):

$$\frac{da}{dN} = A[\Delta K_{eq}(a)]^n \quad (3)$$

where $a$ is the crack length, $N$ is the number of cyclic loads, $\Delta K_{eq}$ is the equivalent SIF at crack tip varied with load cycle, and $A$ and $n$ are material constants or calibration factors.

The correct way to determine the fracture parameters of a material ($A$ and $n$) is to study crack growth of hot mix asphalt (HMA) beam samples under repeated loading conditions, which is a tedious and expensive operation (Francken 1993). Therefore, in this study, $A$ and $n$ values were selected as $3.44\times10^{-6}$ and 2.71, respectively, based on a comprehensive study carried out by Jacob (1995). In addition, it is worthy of note that these values were used by many researchers for simulating the TDC in asphalt pavement (Luo et al. 2010; Modarres and Shabani, 2015). The use of Paris law equation is generally accepted among researchers for description of the rate of crack growth in flexible pavements (Elseifi et al. 2018). By integrating Equation (2), the number of load repetitions ($N_f$) which causes the increase in crack depth (from an initial depth of $a_i$ to a final depth of $a_f$), was computed by:



$$N_f = \int_{a_i}^{a_f} \frac{da}{A[\Delta K_{eq}(a)]^n} \quad (4)$$

Based on the calculated Modes I and II SIF, the equivalent SIF ($\Delta K_{eq}$) was obtained by using (Meggiolaro et al. 2005):

$$\Delta K_{eq} = \sqrt{K_I^2 + K_{II}^2} \quad (5)$$

Regarding that the pavement structures (listed in Table 1), a large number of FE analyses were conducted to investigate the effect of vehicle speed (loading frequency), temperature, crack position, crack depth, AC thickness and base layer type on TDC propagation. The values of KI, KII and fatigue life of the TDC propagation ($N_f$) are presented in the next section.

## Results and discussion

Modes I and II stress intensity factors (KI and KII) of surface-initiated TDC were estimated at 9 transverse locations, ranging from the middle of dual tires to a distance of 250 cm. Due to the symmetric boundary condition at the center of dual tires, only the responses at one side were considered. The 0 transverse distance represents the middle point of the dual tires and 25 transverse distance represents the tire edge at farther distance from the center of dual tires. It should be pointed out that KII contributes to crack growth apart from its sign but only positive value of KI is indicative of crack propagation.

The influence of four AC temperatures (5, 15, 25 and 35°C) on Modes I and II SIFs (KI and KII) are shown in Figures 3 and 4, respectively. As it can be seen, at different locations of TDC, the magnitude of KII and absolute value of KI decrease at elevated temperatures. Furthermore, the magnitudes of KI and KII are significantly affected by TDC location. The maximum value of KII occurs at the tire edge (25 cm transverse distance), while the maximum absolute value of KI is observed at the middle of dual tire (0 cm transverse distance). When the transverse distance of TDC relative to the loading center is within the range of 0 to 50 cm, KI is always negative and KII is the predominant type of SIF; this indicates that that TDC propagation is related to the sliding mode. By increasing the transverse distance of TDC to 75 cm, KI becomes positive and at the same time KII decreases exponentially. Thus, TDC growth is correlated to the combination of Modes I and II of fracture toughness at the corresponding location. At farther transverse distances of TDC (within the distance range of 100 to 250cm), Mode II SIF is almost negligible and the opening mode (KI) becomes gradually dominant. The results show that dual tires loading causes significant shear SIF at the tire edges and for accurate justifying the mechanisms of TDC propagation, the opening mode (KI) and the shear mode (KII) should be considered simultaneously. Although under a single tire loading the Mode II SIF has been neglected in some cases due to its trivial value (Fakhri et al., (2009)), the results of present work show the dual tires effects on Mode II SIF and its contribution to TDC growth; i.e. single tire load is incapable of explaining the real conditions of the cracks at pavement surface under dual tires loading.

In Figures 5 and 6, the variations of KI and KII are plotted for a thick AC thickness (30 cm) based on the TDC depths at 25°C. As it can be seen, when TDC is at the middle of dual tires, the magnitude of KII is 0 at various crack depths and KI is also negative due to the downward deformation. Accordingly, the crack tip at the corresponding location is under compression and it cannot propagate under traffic loading. However, in other transverse locations where the magnitude of KI is negative, the shear deformation (KII) causes the crack propagation. It can be also observed that the crack at 125 cm transverse distance is subjected to a combination of Mode I and II deformation; however, its contribution to TDC growth is less than pure Modes I and II in other locations. In order to clearly illustrate how KI and KII vary with depth, the analysis results are presented in Figures 7 and 8. By increasing TDC depth from 10 to 40 mm, Mode II and absolute value of Mode I SIFs increase especially at close distances to the tire edge. This reveals that the rate of crack growth increases by an increase in crack depth.

Influence of three different AC thicknesses (10, 20 and 30 cm) on variations of KI and KII is presented in Figures 9 and 10 for a TDC with a depth of 40 mm. As it can be observed, by increasing the AC thickness, KI and KII values decrease. However, these changes are more noticeable for mode II SIF at the tire edge (25 cm transverse distance) and mode I SIF at the distance range of 50 to 125 cm away from the loading center. The SIF results show that the thin AC layer is more susceptible to TDC propagation and using of thicker AC layer decreases the likelihood of TDC growth; on the other hand, Baladi et al. (2003) demonstrated that the TDC propagation is independent of the AC thickness.

In order to study the effect of loading frequency on TDC propagation, the analysis was conducted on the pavement with a thin AC layer and a crack depth of 10 mm at various speeds of 10, 40, 80 and 120 km/h. Modes I and II SIF profiles are plotted in Figures 11 and 12, respectively. As it can be observed, by increasing the vehicle speed from 10 to 120 km/h the absolute value of KI increases continuously, whereas the vehicle speed shows insignificant effect on the magnitude of KII. Since the influence of vehicle speed is more pronounced in Mode I SIF, the maximum value of KI is larger than that of KII. According to the results presented in Figure 11 and Figure 3, increasing the loading frequency has the similar effect on the magnitude of KI as decreasing the temperature.

TDC propagation rate in thick AC layer (30 cm) was also evaluated where it was placed on two base layers types; granular base (GB) and cement-treated base (CTB). It was assumed that these layers (i.e., GB and CTB) are isotropic, homogenous and linear elastic materials with different elastic moduli and Poisson ratios. The values of SIF presented in Figures 13 and 14 demonstrate that the pavements with GB are more sensitive to crack growth. In addition, TDC propagation is only due to KI at far transverse distances from the dual tire center (larger than 75 cm) in the pavements with GB, whereas within the transverse distance range of 0 to 75 cm, KII is dominant.

In order to investigate the influence of TDC location on the pavement fatigue life, Paris law model (Eq. (4)) was employed for the prediction of fatigue crack growth rate. The analysis was performed on a thick (30 cm) AC layer at a temperature of 15°C. Since the TDC does not propagate at the middle of dual tire due to the negative value of KI and 0 value of KII, the crack growth rate at the corresponding location is not computed. For other locations, TDC propagation rate is computed from the equivalent SIF ($K_{eq}$). Using the quadratic trend functions (Table 2), $K_{eq}$ is estimated from the crack depth (x). These functions are then utilized in Equation (3) and the integrals are computed by Simpson method. The number of load repetitions to propagate the crack depth from 10 to 50 mm at different TDC locations are shown in Figure 15 (a) and (b). By increasing the crack depth, the number of load repetitions for propagation of TDC decline at different TDC positions. As it can be seen the TDC at the position of P1 (transverse distance of 25 cm) has the most critical condition due to the minimum number of load repetitions. This finding indicates that the TDC propagation rate at the tire edge is significantly higher than that in other locations. Moreover, there is a tremendous rise in maximum fatigue life from $2.5\times10^5$ to $67.7\times10^5$ loading cycles when the transverse distance of TDC increases from 25 to 75 cm (P1 to P3), respectively. In contrast, the maximum fatigue life decreases from $64.4\times10^7$ to $1.5\times10^7$ loading cycles by increasing the distance from 100 to 200 cm (P4 to P7), respectively. Therefore, the position of P4 is not in the critical condition in terms of crack growth rate.

## Conclusions

The cracks at the pavement surface experience tensile and shear deformations, considering one of SIF modes, and assumption of a single tire loading cannot explain the real situation of pavement accurately. Therefore, in this study, numerous finite element analyses were conducted to investigate the dual tires loading effects on longitudinal TDC growth and fatigue life of pavement on the basis of fracture parameters. Based on the analysis results, the following bullets summarize findings from this study:

-The critical values of shear deformation (KII) at the edge of tire and opening deformation (KI) away from the edges of the tire are the driving mechanisms for the propagation of TDC under the dual tires loading. Therefore, the position of TDC relative to the centre of dual tires is a significant factor on variations of magnitude and sign of SIFs.

- By considering temperature gradient, TDC propagation rate at low temperature is faster than that at medium and high temperature due to the larger values of shear and tensile modes.

-By increasing the crack depth, the crack growth rate increases and noticeable changes occur when the crack is located at the tire edge.

-Based on KI and KII results, the thin AC layer is more vulnerable to TDC propagation and using of thick AC layer decreases the likelihood of TDC growth.

-The absolute values of Mode I SIF become larger when the vehicle speed increases, while the speed variations affect the Mode II SIF insignificantly.

-According to the tensile and shear modes of SIF, pavements with GB are more prone to TDC growth than the pavement with CTB.

-By increasing the crack depth, the number of load repetitions for the crack propagation decline at different TDC distances. In addition, TDC at the tire edge has the most critical condition due to the minimum number of load repetitions.

**Acknowledgments**

This research was sponsored by National Natural Science Foundation of China [grant number 51678114], Inner Mongolia Transportation Research Project [grant number NJ-2014-21], Liaoning Transportation Research Project [grant number 201309] and Shanxi Transportation Research Project [grant number 2015-1-22]. The authors gratefully acknowledge their financial support.



**Reference**

Aliha, M. R. M., Bahmani, A., & Akhondi, S. 2016. A novel test specimen for investigating the mixed mode I+ III fracture toughness of hot mix asphalt composites–Experimental and theoretical study. International Journal of Solids and Structures, 90, 167-177.

Al-Qadi, I. L., Elseifi, M. A., & Yoo, P. J. 2004. Pavement damage due to different tires and vehicle configurations. Virginia Tech Transportation Institute, VA, USA.

Al-Qadi, I.L., Xie, W. and Elseifi, M.A. 2008. Frequency Determination from Vehicular Loading Time Pulse to Predict Appropriate Complex Modulus in MEPDG. Journal of the Association of Asphalt Paving Technologists, Vol. 77, 739-772.

Ameri, M., Mansourian, A., Khavas, M. H., Aliha, M. R. M., & Ayatollahi, M. R. 2011.

Cracked asphalt pavement under traffic loading–A 3D finite element analysis. Engineering Fracture Mechanics, 78(8), 1817-1826.

American Association of State Highway and Transportation officials (AASHTO), 2007. “Standard method of test for determining dynamic modulus of hot-mix asphalt (HMA).” AASHTO TP 62-07, Washington, DC.

Applied Research Associates (ARA) 2004.” Guide for Mechanistic-Empirical Design of New and Rehabilitated Pavement Structures.” Final Report, National Cooperative Highway Research Program (NCHRP) Project 1-37A, Albuquerque, New Mexico.

Archilla, A. R. 2015. Top-Down Fatigue Cracking in High-Temperature Environments. Transportation Research Record: Journal of the Transportation Research Board, (2507), 128-137.

Baladi, G. Y., Schorsch, M., & Svasdisant, T. 2003. Determining the causes of top-down cracks in bituminous pavements (No. RC-1440).

Bayomy, F., Mull-Aglan, M. A., Abdo, A. A., & Santi, M. J. 2006. Evaluation of hot mix asphalt (HMA) fracture resistance using the critical strain energy release rate, Jc (No. 06-2745).

Elseifi, M. A., Baek, J., & Dhakal, N. 2018. Review of modelling crack initiation and propagation in flexible pavements using the finite element method. International Journal of Pavement Engineering, 19(3), 251-263.

Fakhri, M., Farokhi, M., & Kheiry, P. T. 2009. Modeling of top-down cracking (TDC) propagation in asphalt concrete pavements using fracture mechanics theory. Adv Test Charact Bituminous Mater II, 681-692.

Holewinski, J. M., Soon, S., Drescher, A., & Stolarski, H. K. 2003. Investigation of factors related to surface-initiated cracks in flexible pavements, USA: Department of Civil Engineering, University of Minnesota.

Huang, B., Shu, X., & Zuo, G. 2013. Using notched semi circular bending fatigue test to characterise fracture resistance of asphalt mixtures. Engineering Fracture Mechanics, 109, 78-88.

Jacobs, M. M. J., Hopman, P. C., & Molenaar, A. A. A. 1996. Application of fracture mechanics principles to analyze cracking in asphalt concrete (with discussion). Journal of the Association of Asphalt Paving Technologists, 65.

Kim, H., Wagoner, M. P., & Buttlar, W. G. 2009. Micromechanical fracture modeling of asphalt concrete using a single-edge notched beam test. Materials and Structures, 42(5), 677.

Li, X., Zofka, A., Marasteanu, M., & Clyne, T. R. 2006. Evaluation of field aging effects on asphalt binder properties. Road Materials and Pavement Design, 7(sup1), 57-73.

Ling, M., Luo, X., Gu, F., & Lytton, R. L. 2017a. An inverse approach to determine complex modulus gradient of field-aged asphalt mixtures. Materials and Structures, 50(2), 138.

Ling, M., Luo, X., Hu, S., Gu, F., & Lytton, R. L. 2017b. Numerical modeling and artificial neural network for predicting J-integral of top-down cracking in asphalt pavement. Transportation Research Record: Journal of the Transportation Research Board, (2631), 83-95.

Luo, H., Zhu, H. P., Miao, Y., & Chen, C. Y. 2010. Simulation of top-down crack propagation in asphalt pavements. Journal of Zhejiang University-Science A, 11(3), 223-230.

Luo, X., Gu, F., Ling, M., & Lytton, R. L. 2018. Review of mechanistic-empirical modeling of top-down cracking in asphalt pavements. Construction and Building Materials, 191, 1053-1070.

Matsuno, S., & Nishizawa, T. 1992. Mechanism of longitudinal surface cracking in asphalt pavement. Proceeding of 7th International Conference on Asphalt Pavements, The University of Nottingham (pp. 277– 291), August 13–15.

Meggiolaro, M. A., Miranda, A. C. O., Castro, J. T. P., & Martha, L. F. 2005. Stress intensity factor equations for branched crack growth. Engineering Fracture Mechanics, 72(17), 2647-2671.

Modarres, A., & Shabani, H. 2015. Investigating the effect of aircraft impact loading on the longitudinal top-down crack propagation parameters in asphalt runway pavement using fracture mechanics. Engineering Fracture Mechanics, 150, 28-46.

Molenaar, J. M. M., Liu, X., & Molenaar, A. A. A. 2003, April. Resistance to crack-growth and fracture of asphalt mixture. In 6th International RILEM Symposium on Performance Testing and Evaluation of Bituminous Materials, Zurich, Switzerland (pp. 618-625).

Myers, L. A., & Roque, R. 2002. Top-down crack propagation in bituminous pavements and implications for pavement management. Journal of the Association of Asphalt Paving Technologists, 71.

Niederquell, M., Baladi, G., & Chatti, K. 2000. Rubblization of concrete pavements: Field investigation. Transportation Research Record: Journal of the Transportation Research Board, (1730), 150-160.

Paris, P. C., & Erdogan, F. 1963, December. A critical analysis of crack propagation laws. ASME.

Raju, S., Kumar, S. S., Reddy, K. S., Bose, S., & Pandey, B. B. 2008. Analysis of Top-Down Cracking Behavior of Asphalt Pavements. Transportation Research Board, Washington, D.C.

Rashadul Islam, M., Vallejo, M. J., & Tarefder, R. A. 2016. Crack propagation in hot mix asphalt overlay using extended finite-element model. Journal of Materials in Civil Engineering, 29(5), 04016296.

Roesler, J., & Khazanovich, L. 1997. Finite-element analysis of Portland cement concrete pavements with cracks. Transportation Research Record: Journal of the Transportation Research Board, (1568), 1-9.

Shen, S., Zhang, W., Wang, H., & Huang, H. 2017. Numerical evaluation of surface-initiated cracking in flexible pavement overlays with field observations. Road Materials and Pavement Design, 18(1), 221-234.

Sun, L., & Hudson, W. R. 2005. Probabilistic approaches for pavement fatigue cracking prediction based on cumulative damage using Miner's law. Journal of engineering mechanics, 131(5), 546-549.

Svasdisant, T., Schorsch, M., Baladi, G., & Pinyosunun, S. 2002. Mechanistic analysis of top down cracks in asphalt pavements. Transportation Research Record: Journal of the Transportation Research Board, (1809), 126-136.

Wang, P. 2009. The Research on Mechanism of Surface Cracking in Asphalt Pavement. Southeast University, China.

Wang, H., Ozer, H., Al-Qadi, I. L., & Duarte, C. A. 2013. Analysis of near-surface cracking under critical loading conditions using uncracked and cracked pavement models. Journal of Transportation Engineering, 139(10), 992-1000.

Yang, B., Huang, Q. S., Xiong, B., & Xu, H. 2011. Analysis on the Effect of Parameters Variation on Dynamic Stress Intensity Factor of Asphalt Overlay Reflective Crack. In Applied Mechanics and Materials (Vol. 52, pp. 1092-1096). Trans Tech Publications.

Zhao, Y., Ni, F., & Zhou, L. 2011. Viscoelastic response of reflective cracking under dynamic vehicle loading in asphalt concrete pavements. In ICCTP 2011: Towards Sustainable Transportation Systems (pp. 3278-3297).

Zhao, Y., Liu, H., Bai, L., & Tan, Y. 2012. Characterization of linear viscoelastic behaviour of asphalt concrete using complex modulus model. Journal of Materials in Civil Engineering, 25(10), 1543-1548.

Zhao, Y., Alae, M., & Fu, G. 2018. Investigation of mechanisms of top-down fatigue cracking of asphalt pavement. Road Materials and Pavement Design, 19(6), 1436-1447.

Zhao, K., & Wang, Y. 2018. Influences of aging conditions on the rheological properties of asphalt binders. International Journal of Pavement Engineering, 1-13.

**List of tables**



**List of figures**

Figure 11. The influence of vehicle speed on Mode I SIF with a crack depth of 10 mm.

Figure 12. The influence of vehicle speed on Mode II SIF with a crack depth of 10 mm.

Figure 13. The influence of base type on Mode I SIF with a crack depth of 30 mm.

Figure 14. The influence of base type on Mode II SIF with a crack depth of 30 mm.

Figure 15. Number of load repetition for TDC propagation: (a) within the distance range of 25 to 75 cm; (b) within the distance range of 100 to 200 cm.

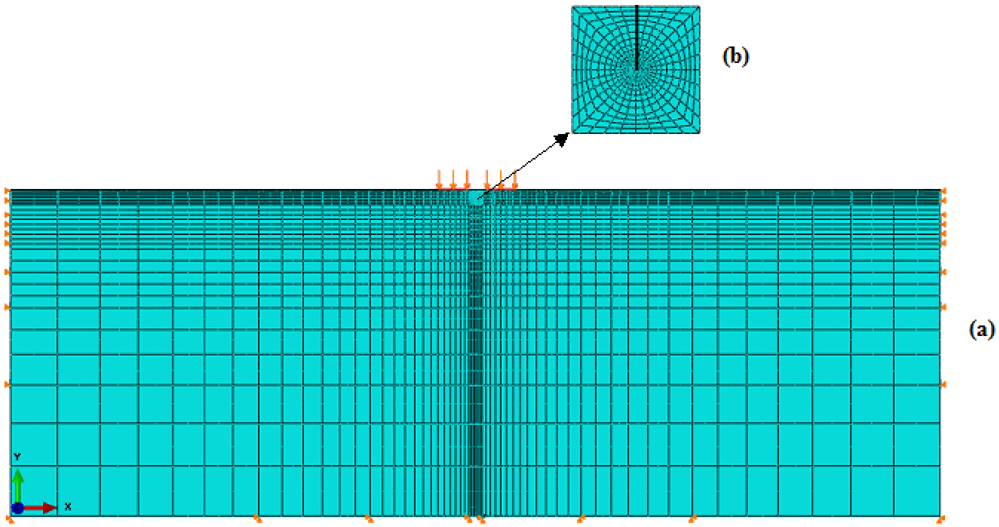
(b)
(a)
Y
X

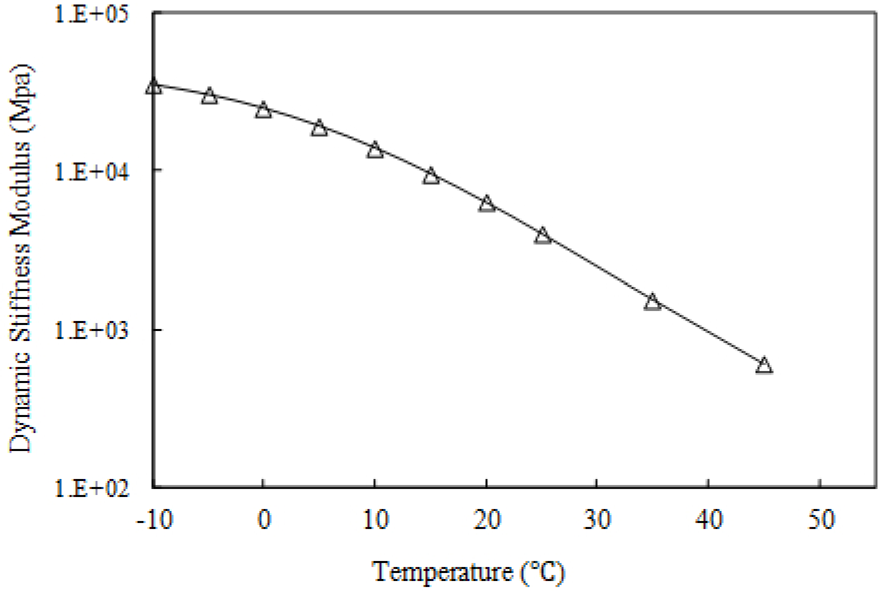
1.E+05
1.E+04
1.E+03
1.E+02
Dynamic Stiffness Modulus (Mpa)
-10
0
10
20
30
40
50
Temperature (°C)

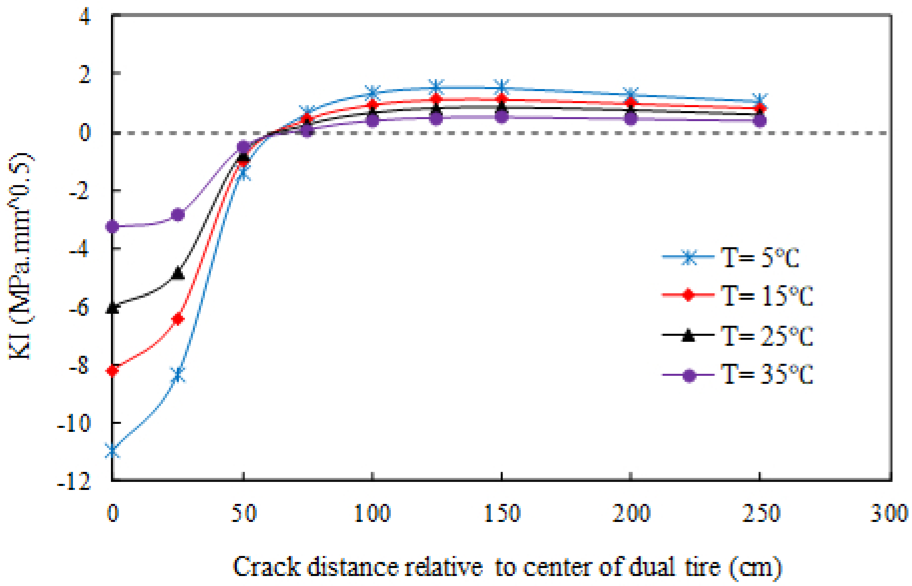
KI (MPa.mm^0.5)
4
2
0
-2
-4
-6
-8
-10
-12
0
50
100
150
200
250
300
Crack distance relative to center of dual tire (cm)
T= 5°C
T= 15°C
T= 25°C
T= 35°C

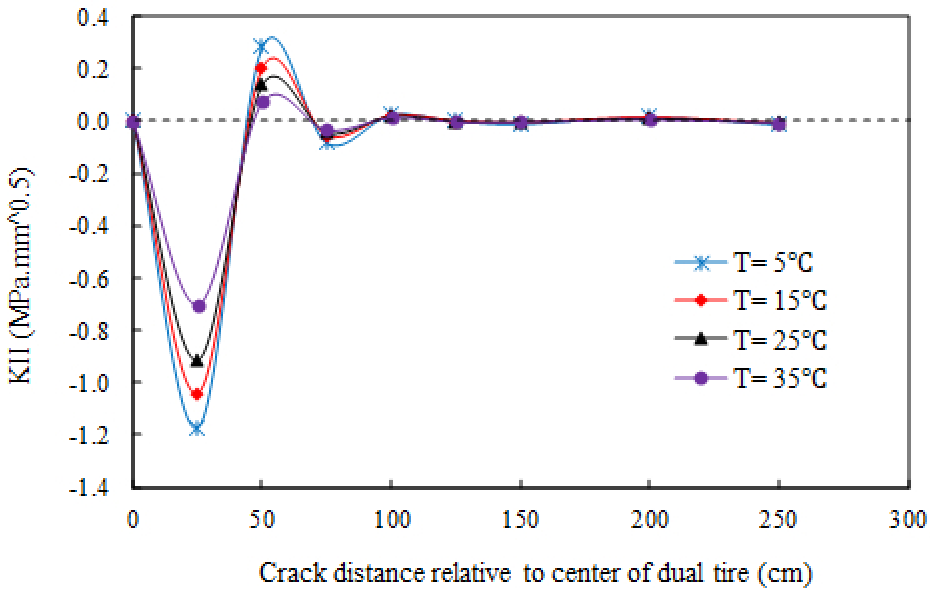
0.4
0.2
0.0
-0.2
-0.4
-0.6
-0.8
-1.0
-1.2
-1.4
0
50
100
150
200
250
300
KII (MPa.mm^0.5)
Crack distance relative to center of dual tire (cm)
T= 5°C
T= 15°C
T= 25°C
T= 35°C

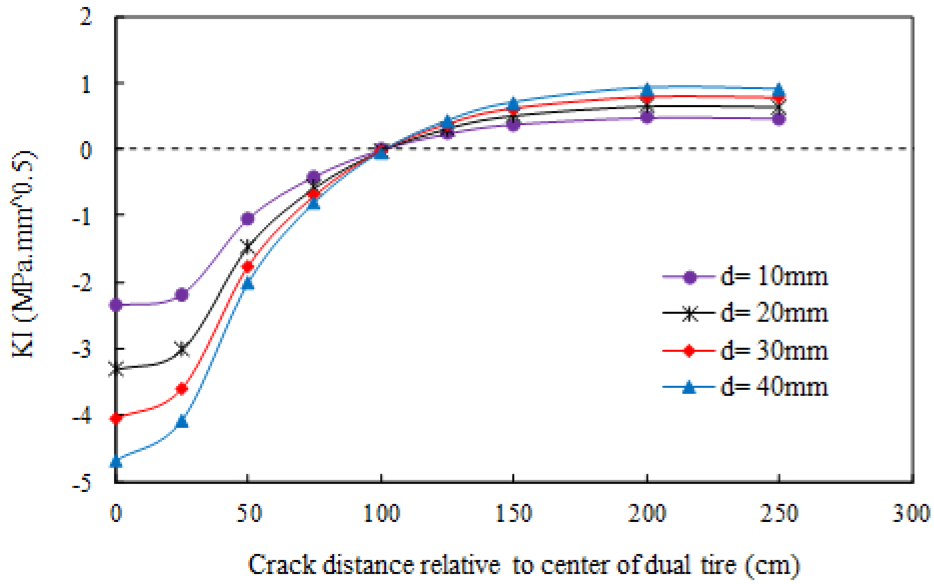
KI (MPa.mm^0.5)
Crack distance relative to center of dual tire (cm)
d= 10mm
d= 20mm
d= 30mm
d= 40mm
2
1
0
-1
-2
-3
-4
-5
0
50
100
150
200
250
300

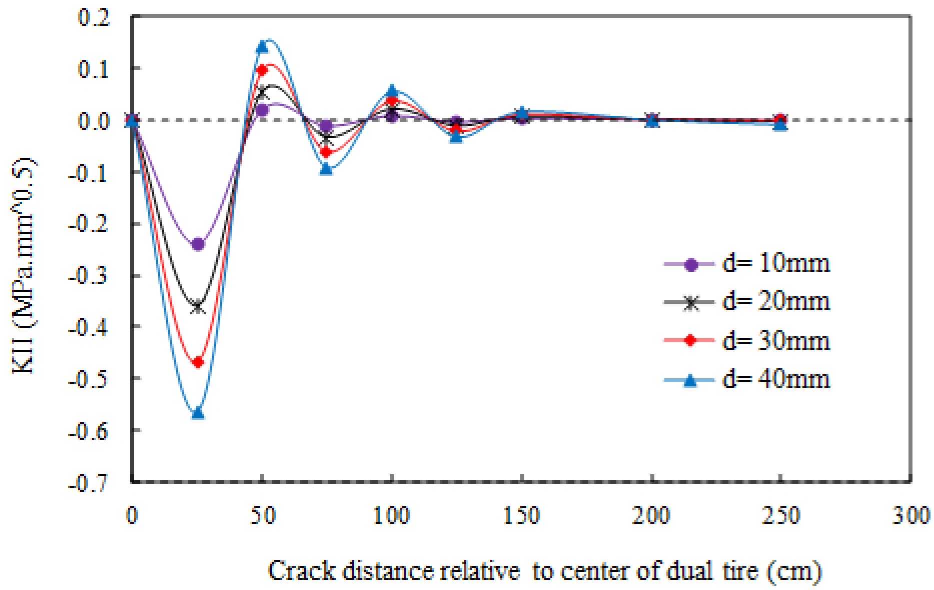
0.2
0.1
0.0
-0.1
-0.2
-0.3
-0.4
-0.5
-0.6
-0.7
KII (MPa.mm^0.5)
d= 10mm
d= 20mm
d= 30mm
d= 40mm
0
50
100
150
200
250
300
Crack distance relative to center of dual tire (cm)

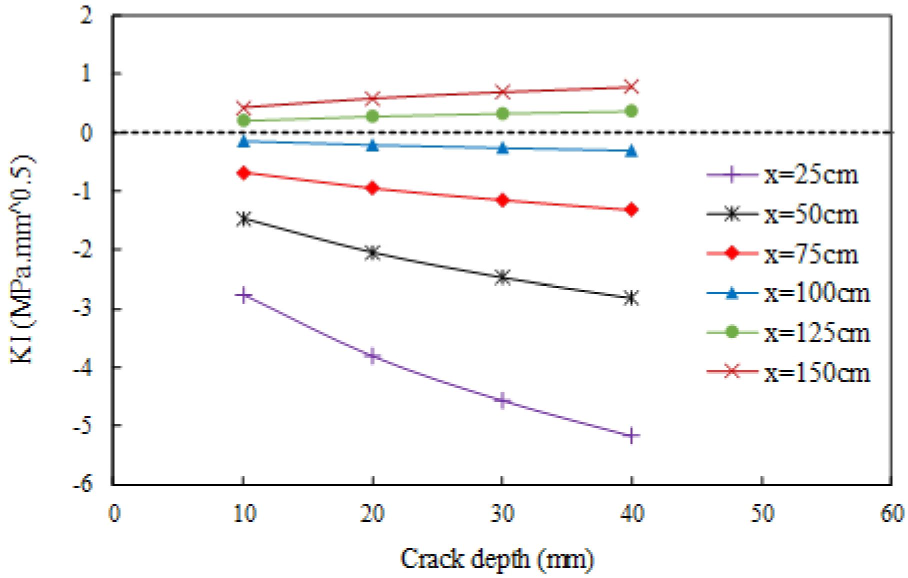
2
1
0
-1
-2
-3
-4
-5
-6
KI (MPa.mm^0.5)
0
10
20
30
40
50
60
Crack depth (mm)
x=25cm
x=50cm
x=75cm
x=100cm
x=125cm
x=150cm

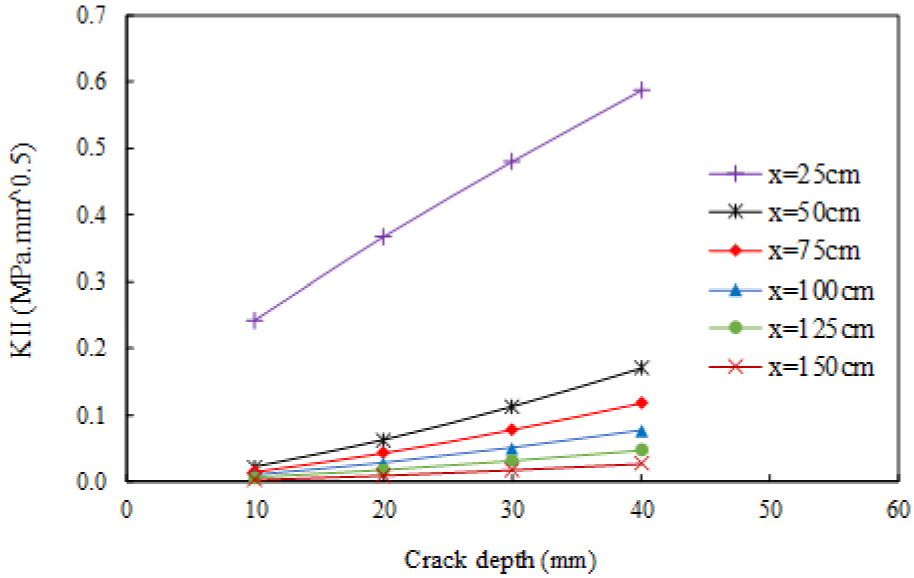
0.7
0.6
0.5
0.4
0.3
0.2
0.1
0.0
KII (MPa.mm^0.5)
0
10
20
30
40
50
60
Crack depth (mm)
x=25cm
x=50cm
x=75cm
x=100cm
x=125cm
x=150cm

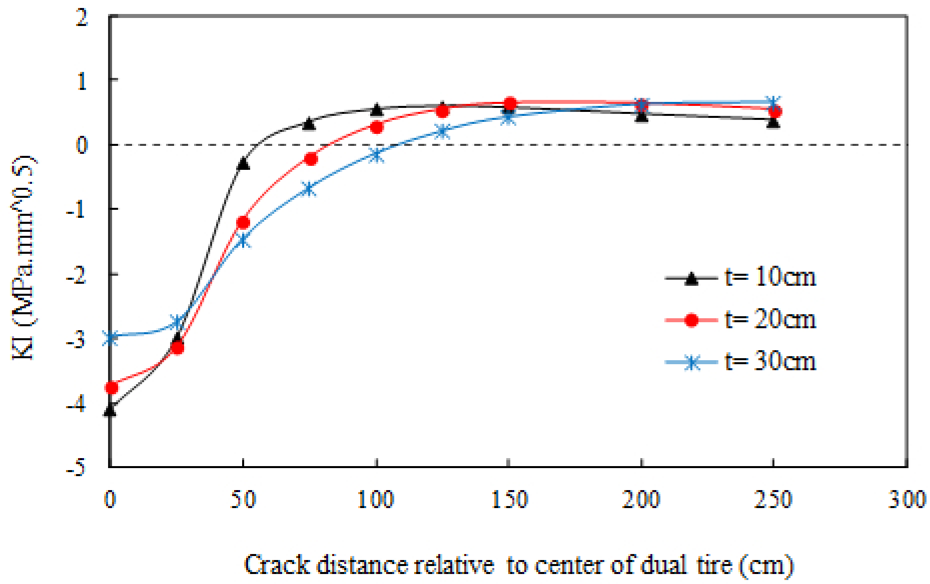
KI (MPa.mm^0.5)
2
1
0
-1
-2
-3
-4
-5
0
50
100
150
200
250
300
Crack distance relative to center of dual tire (cm)
t= 10cm
t= 20cm
t= 30cm

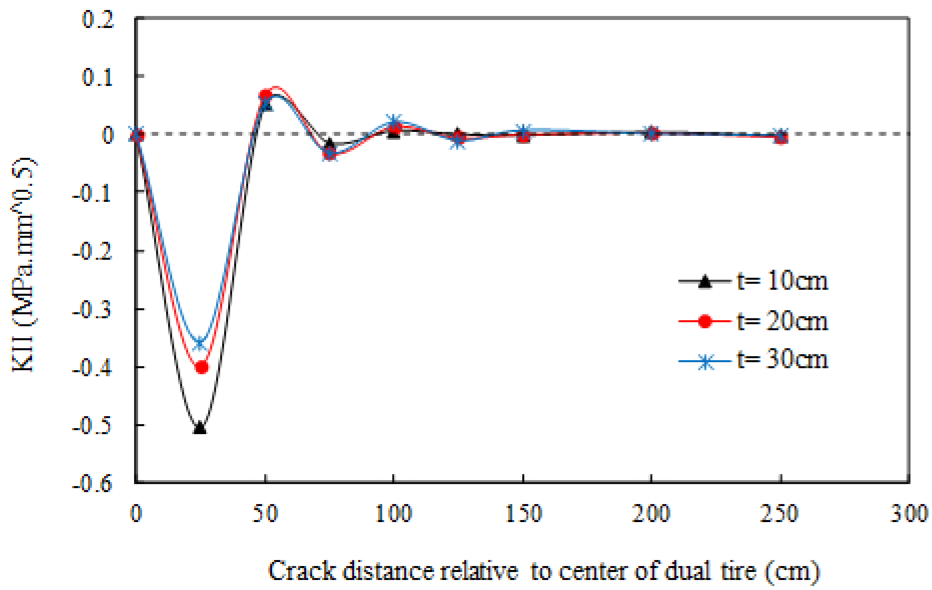
0.2
0.1
0
-0.1
-0.2
-0.3
-0.4
-0.5
-0.6
KII (MPa.mm^0.5)
0
50
100
150
200
250
300
Crack distance relative to center of dual tire (cm)
t= 10cm
t= 20cm
t= 30cm

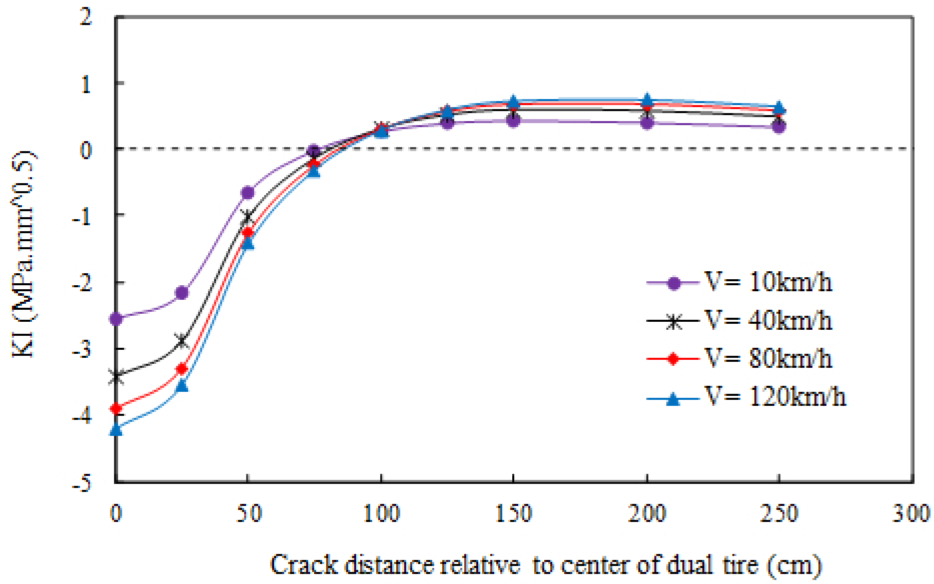
2
1
0
-1
-2
-3
-4
-5
KI (MPa.mm^0.5)
0
50
100
150
200
250
300
Crack distance relative to center of dual tire (cm)
V= 10km/h
V= 40km/h
V= 80km/h
V= 120km/h

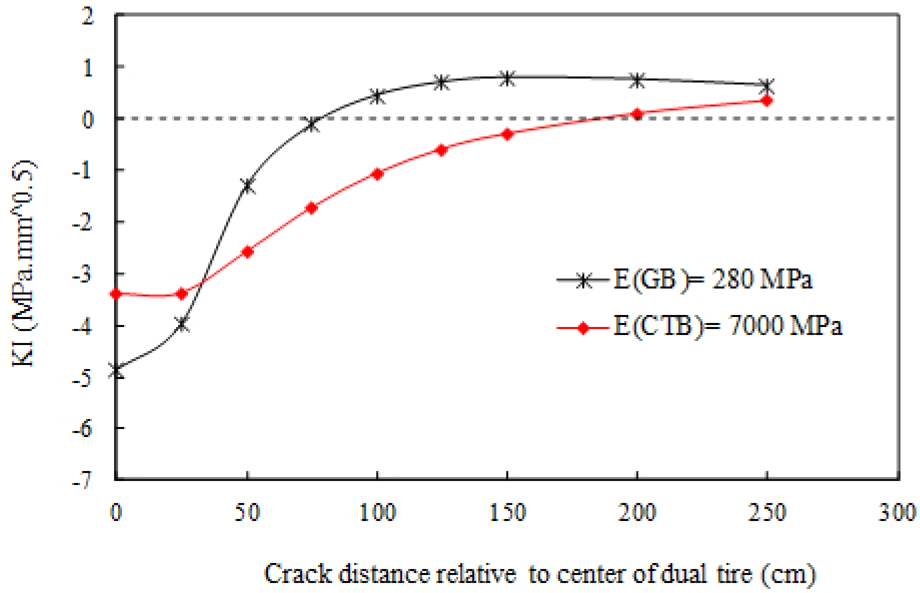
2
1
0
-1
-2
-3
-4
-5
-6
-7
KI (MPa.mm^0.5)
0
50
100
150
200
250
300
Crack distance relative to center of dual tire (cm)
E(GB)= 280 MPa
E(CTB)= 7000 MPa

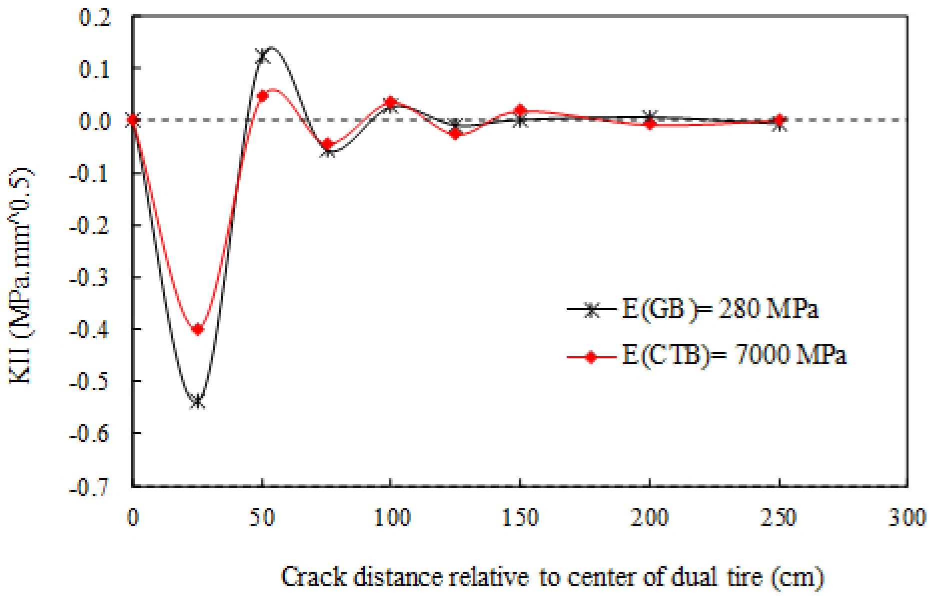
0.2
0.1
0.0
-0.1
-0.2
-0.3
-0.4
-0.5
-0.6
-0.7
KII (MPa.mm^0.5)
E(GB)= 280 MPa
E(CTB)= 7000 MPa
0
50
100
150
200
250
300
Crack distance relative to center of dual tire (cm)

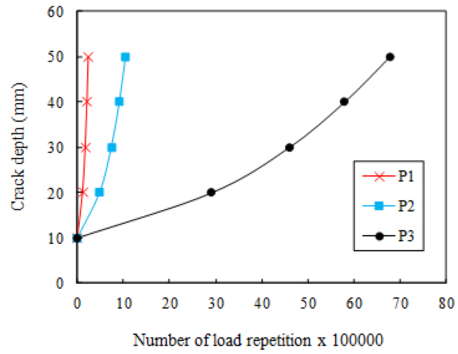
60
50
40
30
20
10
0
Crack depth (mm)
0 10 20 30 40 50 60 70 80
Number of load repetition x 100000
P1
P2
P3

(a)

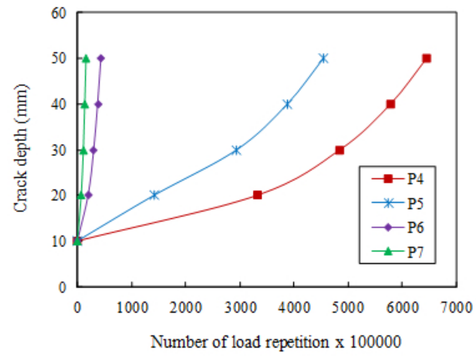
60
50
40
30
20
10
0
Crack depth (mm)
0 1000 2000 3000 4000 5000 6000 7000
Number of load repetition x 100000
P4
P5
P6
P7

(b)